Roles of the color antisymmetric ghost propagator in the infrared QCD

Sadataka Furui, * School of Science and Engineering,
Teikyo University

20 March 2008 St.Goar "Quarks and Hadrons in strong QCD"

*e-mail furui@umb.teikyo-u.ac.jp

Contents

Reference: Prog. Theor. Phys. **119**, 149(2008), arXiv:0709.2804(hep-ph); arXiv:0801.0325(hep-lat)

Collaborator in lattice simulation : H. Nakajima (Utsunomiya-u).

I. Introduction

- Search confinement and chiral symmetry breaking through lattice results of

  1. Gluon propagator

  2. Ghost propagator

  3. Quark propagator

- Compare our lattice results with the Dyson-Schwinger approach and other continuum theories.

  A. Cucchieri, T. Mendes and A. Mihara, Phys. Rev. D**72**,094505(2005),

  Dudal, Vandersickel, Sorella.

- Study Slavnov identity and renormalization à la Zavialov (*Renormalized Quantum Field Theory*, Kluwer Academic Pub. 1990).

- 我田引水 Draw other's water into one's own farm.

Landau gauge

- The minimizing function of the Landau gauge($\partial_\mu A_\mu = 0$)

  1. $\log U$ type: $U_{x,\mu} = e^{A_{x,\mu}},\ A^\dagger_{x,\mu} = -A_{x,\mu}$,
     $F_U(g) = ||A^g||^2 = \sum_{x,\mu} \mathrm{tr}\left({A^g}_{x,\mu}{}^\dagger A^g_{x,\mu}\right)$,

  2. U linear type: $A_{x,\mu} = \frac{1}{2}(U_{x,\mu} - {U_{x,\mu}}^\dagger)|_{trlp.}$,
     $F_U(g) = \sum_{x,\mu} \mathrm{tr}\left(2 - (\ U^g_{x,\mu} + {U^g_{x,\mu}}^\dagger)\right)$,

- Gauge uniqueness: Fundamental modular region

Coulomb gauge

- The minimizing function of the Coulomb gauge($\partial_i A_i = 0$)

  1. Log-U: $F_U[g] = ||\boldsymbol{A}^g||^2 = \sum_{x,i} \mathrm{tr}\left({A^g}_{x,i}{}^\dagger A^g_{x,i}\right)$,

  2. U-linear: $F_U[g] = \sum_{\boldsymbol{x},i=1,2,3} tr(2 - ({U^g}_i(\boldsymbol{x},t) + {U^{g\dagger}}_i(\boldsymbol{x},t))$
     where ${U^g}_i(x) = g(x)U_i(x)g^\dagger(x+i)$.

- Remnant gauge fixing : The gauge field $A_0(x)$ can be fixed by the following minimizing function of $g(x_0)$.

  1. Log-U: $F_U[g] = ||{A^g}_0||^2 = \sum_x \mathrm{tr}\left({A^g}_{x,0}{}^\dagger A^g_{x,0}\right)$,

  2. U-linear:$F_U[g] = \sum_{\boldsymbol{x}} tr(2 - ({U^g}_0(\boldsymbol{x},t) + U_0^{g\dagger}(\boldsymbol{x},t))$

Landau gauge ghost propagator

$$\begin{aligned} FT[D_G^{ab}(x,y)] &= FT\langle tr(\Lambda^a\{(\mathcal{M}[U])^{-1}\}_{xy}\Lambda^b\rangle, \\ &= \delta^{ab}D_G(q^2), \end{aligned}$$

$$\mathcal{M} = -\partial_\mu D_\mu.$$

- Ghost dressing function $G(q^2) = q^2 D_G(q^2)$.

- Solve the equation with plane wave sources.

$$-\partial_\mu D_\mu f_s^b(x) = \frac{1}{\sqrt{V}}\Lambda^b \sin qx \qquad (1)$$

$$-\partial_\mu D_\mu f_c^b(x) = \frac{1}{\sqrt{V}}\Lambda^b \cos qx. \qquad (2)$$

- Color diagonal ghost propagator

$$D_G(q) = \frac{1}{N_c^2 - 1}\frac{1}{V}$$
$$\times\delta^{ab}(\langle\Lambda^a \cos qx|f_c^b(x)\rangle + \langle\Lambda^a \sin qx|f_s^b(x)\rangle) \tag{3}$$

- Color antisymmetric ghost propagator

$$\phi^c(q) = \frac{1}{\mathcal{N}}\frac{1}{V}$$
$$\times f^{abc}(\langle\Lambda^a \cos qx|f_s^b(x)\rangle - \langle\Lambda^a \sin qx|f_c^b(x)\rangle) \tag{4}$$

where $\mathcal{N} = 2$ for SU(2) and 6 for SU(3).

Unquenched configurations

- The Kogut-Susskind fermion (MILC collaboration)

- The domain wall fermion (RBC/UKQCD collaboration)

The parameters of the lattice configurations

	β	N_f	m	$1/a$(GeV)	L_s	L_t	aL_s(fm)
MILC$_{ft1}$	5.65	2	0.008	1.716	24	12	2.76
MILC$_{ft3}$	5.725	2	0.008	1.914	24	12	2.47
MILC$_{ft5}$	5.85	2	0.008	2.244	24	12	2.11
MILC$_c$	6.83(β_{imp})	2+1	0.040/0.050	1.64	20	64	2.41
	6.76(β_{imp})	2+1	0.007/0.050	1.64	20	64	2.41
MILC$_f$	7.11(β_{imp})	2+1	0.0124/0.031	2.19	28	96	2.52
	7.09(β_{imp})	2+1	0.0062/0.031	2.19	28	96	2.52
MILC$_{2f}$	7.20(β_{imp})	2	0.020	1.64	20	64	2.41
MILC$_{3f}$	7.18(β_{imp})	3	0.031	2.19	28	96	2.52
DWF$_{01}$	2.13(β_I)	2+1	0.01/0.04	1.743(20)	16	32	1.81
DWF$_{02}$	2.13(β_I)	2+1	0.02/0.04	1.703(16)	16	32	1.85
DWF$_{03}$	2.13(β_I)	2+1	0.03/0.04	1.662(20)	16	32	1.90

Ghost propagator

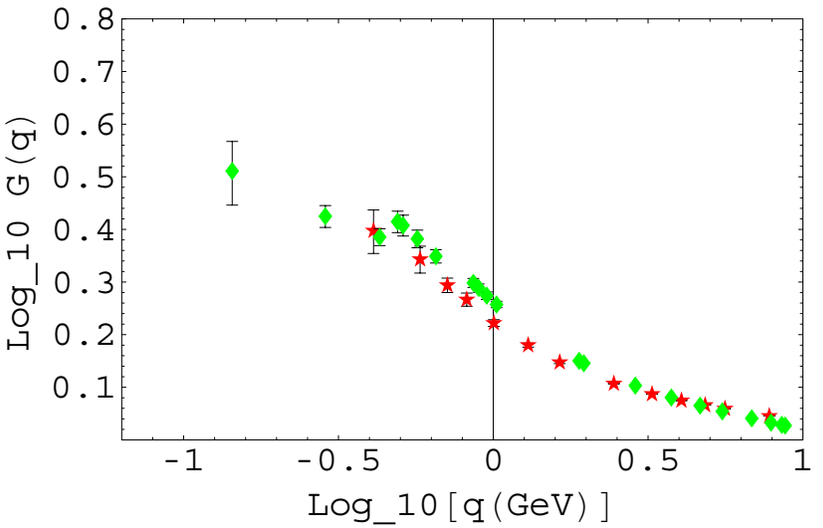

Fig. 1: Log of the ghost dressing function $\log_{10} G(q)$ as a function of $\log_{10} q$(GeV) of MILC$_f$ $\beta_{imp} = 7.09$ (diamonds) and that of quenched $\beta = 6.45$ 56^4 (stars).

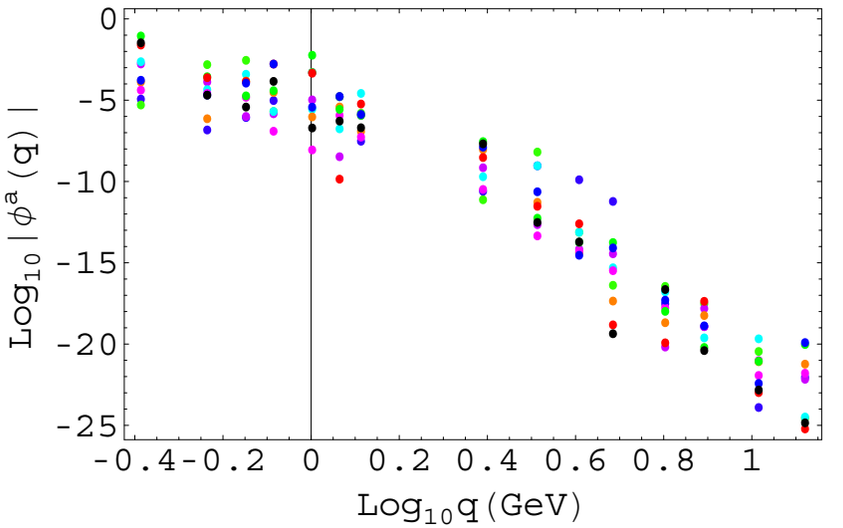

Fig. 2: Log of the color antisymmetric ghost propagator $\log_{10}[D_G(q)]$ as a function of q(GeV). Quenched $\beta = 6.45, 56^4$.

S.F and H. Nakajima, Phys. Rev. **D76**,054509(2007)

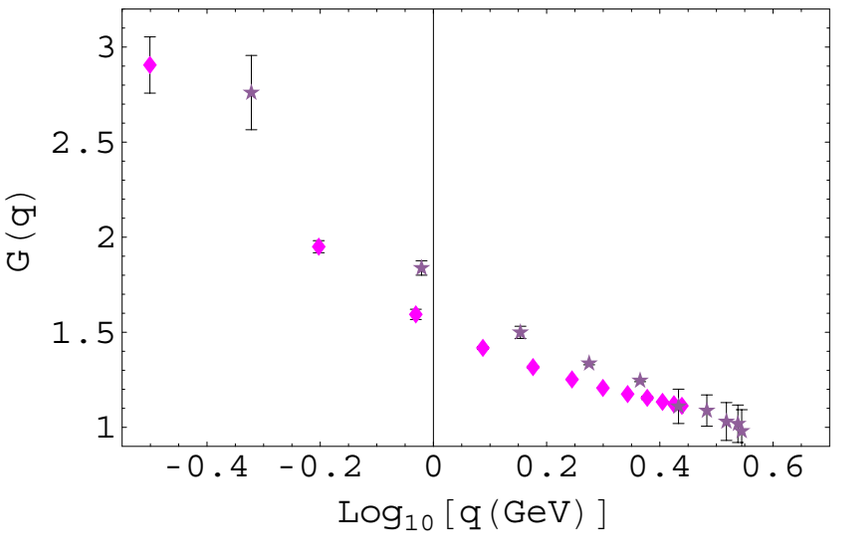

Fig. 3a:The ghost dressing function $G(q)$ of MILC$_{2f}$(violet stars) and that of MILC$_{3f}$(magenta diamonds).

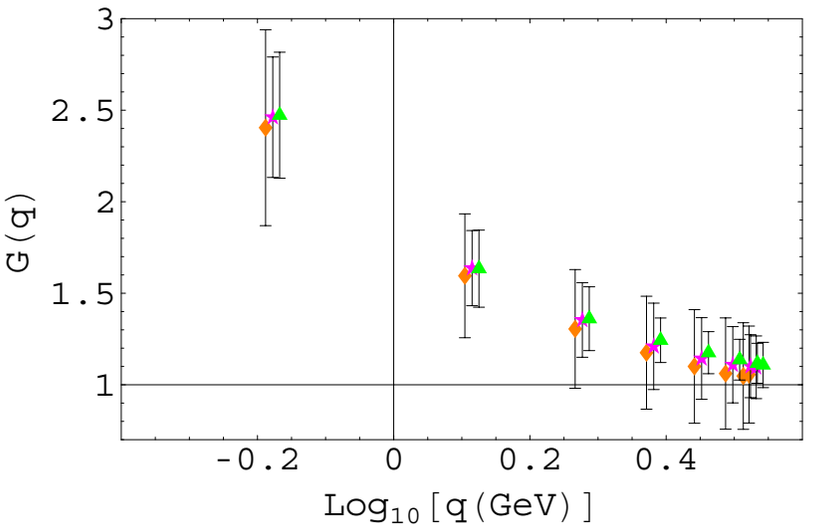

Fig. 3b:The ghost dressing function $G(q)$ of DWF $m = 0.01$(green triangles), 0.02(red stars), 0.03 (blue diamonds).

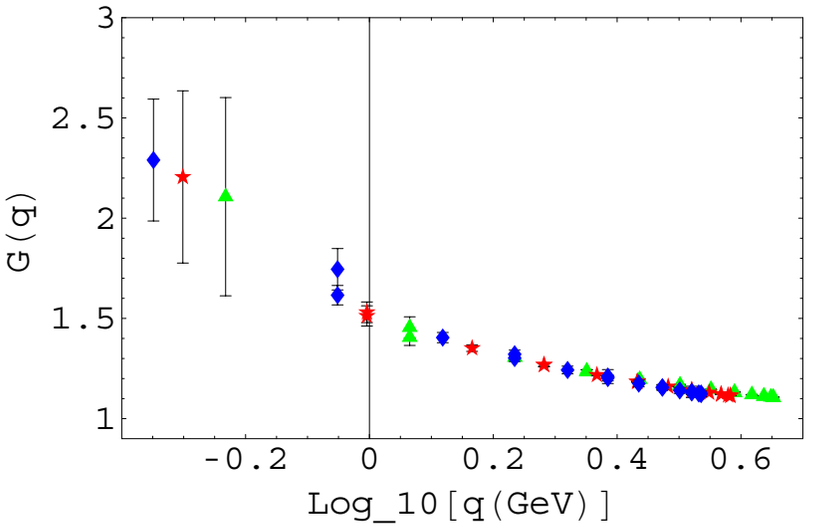

Fig. 4a: Landau gauge ghost dressing function of MILC$_{ft}$ T/T_c = 1.02(blue diamonds), T/T_c = 1.23(red stars) and T/T_c = 1.32(green triangles).)

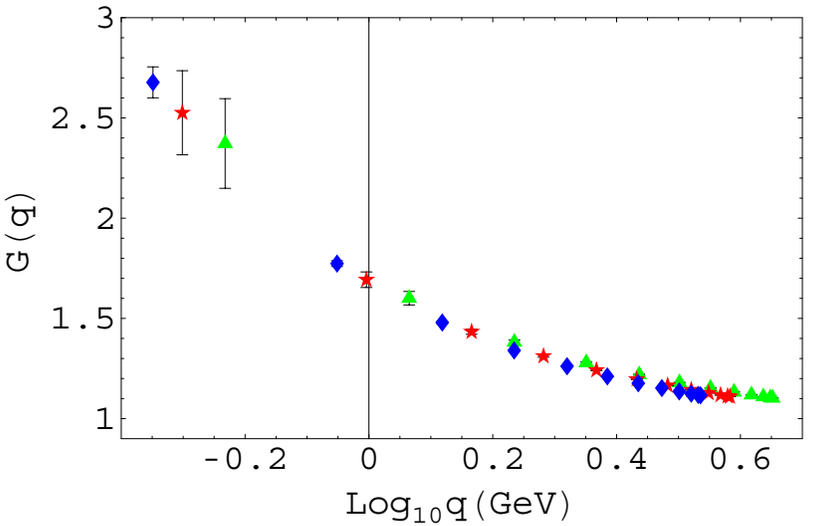

Fig. 4b: Coulomb gauge ghost dressing function of MILC$_{ft}$ T/T_c = 1.02(blue diamonds), T/T_c = 1.23(red stars) and T/T_c = 1.32(green triangles).)

String tension is not a good indication of the confinement. Greensite

S.F and H. Nakajima, Phys. Rev. **D76**,054509(2007)

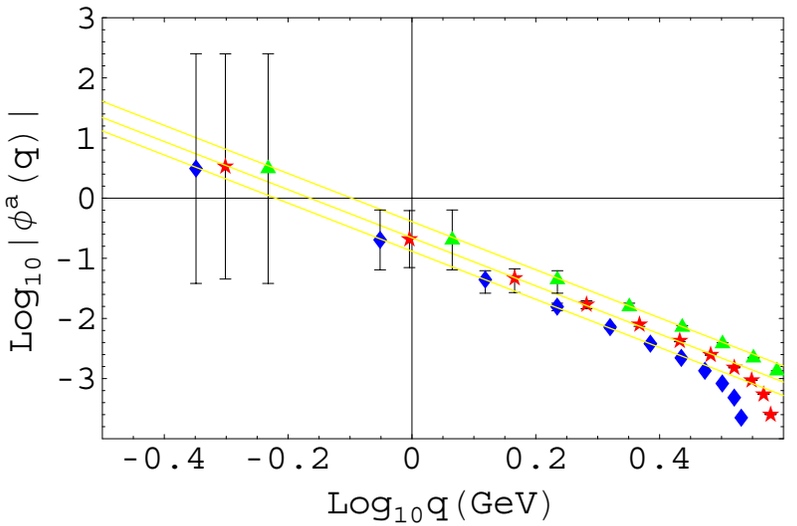

Fig. 5a:The color antisymmetric ghost propagator $\log|\vec{\phi}(\boldsymbol{q})|$ of MILC$_{ft}$T/T$_c$ = 1.02(blue diamonds), $T/T_c = 1.23$(red stars) and $T/T_c = 1.32$(green triangles).

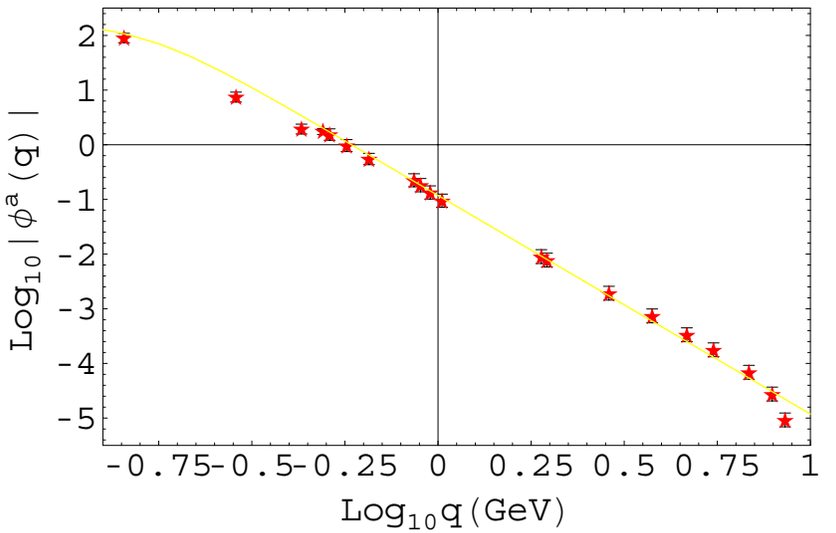

Fig. 5b:$\log_{10}|\vec{\phi}(q)|$ as the function of $\log_{10}(q(\text{GeV}))$ of MILC$_f$ and the fit using $r = 134$ and $v = 0.026\text{GeV}^2$.

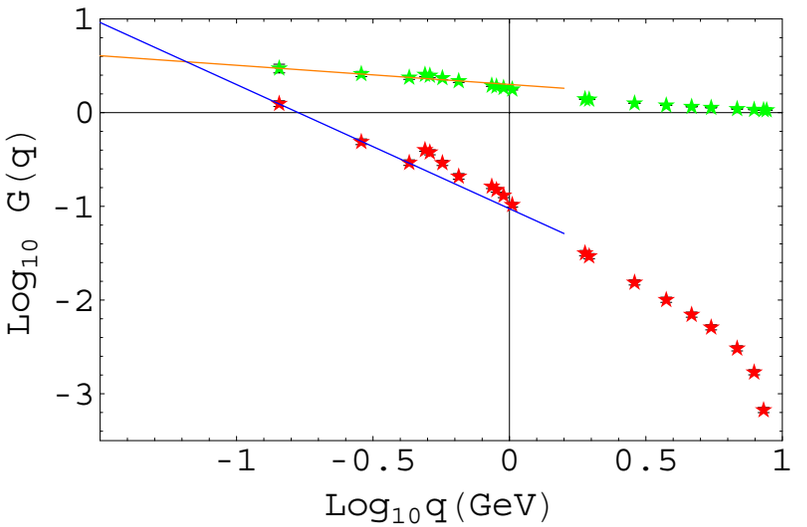

Fig. 6:The color antisymmetric ghost dressing function $\log_{10}(|\phi(q)|q^2)$ (Red) and color diagonal ghost dressing function $\log G(q)$ (Green) of MILC$_{3f}$. Slope defined by the lowest three points of the former is -1.32 and that of the latter is -0.20.

III. The triple gluon and the gh-gl-gh vertex

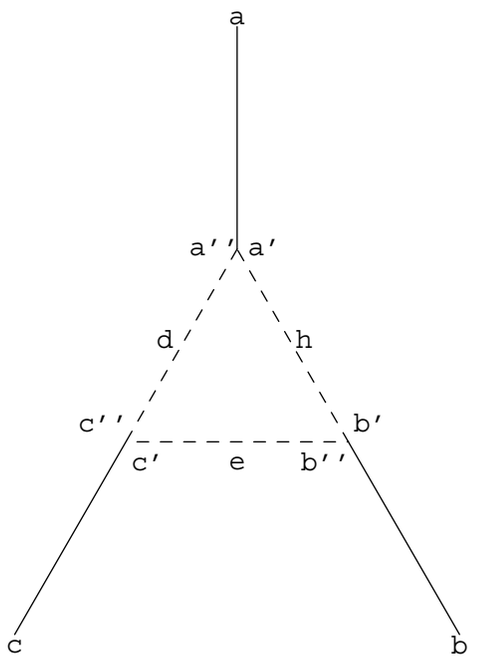

Fig.7: The ghost triangle and the color indices of the external gluons and internal ghosts.

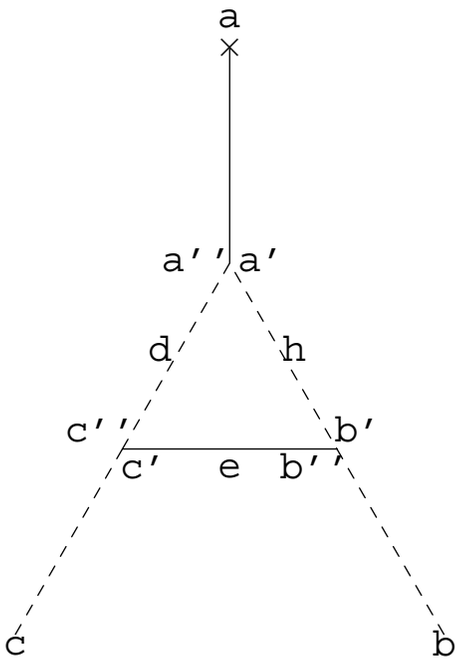

Fig. 8: The ghost-ghost-gluon loop contribution in the ghost-gluon vertex. The dashed line is a ghost the thin line is a gluon.

- We express the ghost propagator, which is assigned as d, as a combination of the color diagonal and color antisymmetric pieces:

$$\delta^{a''c''} D_G(k) + 2 f^{a''c''d} \phi_d(k). \tag{5}$$

- The same combination is assumed for the ghost assigned as h. The color factor

$$f^{a''a'a} f^{b''b'b} f^{c''c'c} \tag{6}$$

is multiplied at the three edges of the triangle.

abc	deh	$D_hD_dD_e$	$D_h\phi_d\phi_e$	$D_d\phi_e\phi_h$	$D_e\phi_h\phi_d$
123	888	-1.5	-1.5	1.5	1.5
	333	-1.5	-4.5	0	0
	833	-1.5	0	-0.5	0
	383	-1.5	0	0	-0.5
	338	-1.5	-4.5	0	0
	838	-1.5	0	0	1.5
	883	-1.5	-1.5	0	0
	388	-1.5	0	1.5	0
147	888	-1.5	0	0	1.5
	333	-1.5	-1	1	-0.5
	338	-1.5	-1	0	$-\sqrt{3}/2$
	383	-1.5	$-\sqrt{3}$	$-\sqrt{3}$	-0.5
	833	-1.5	0	1	$\sqrt{3}/2$
	883	-1.5	0	$-\sqrt{3}$	$\sqrt{3}/2$
	838	-1.5	0	0	1.5
	388	-1.5	$-\sqrt{3}$	0	$\sqrt{3}/2$

Table 1a:The $SU(3)$ color matrix elements of the ghost triangle.

abc	deh	$D_hD_dD_e$	$D_h\phi_d\phi_e$	$D_d\phi_e\phi_h$	$D_e\phi_h\phi_d$
458	888	-1.5	4.5	0	0
	333	-1.5	-1.5	1	1
	338	-1.5	-1.5	0	0
	383	-1.5	$-\sqrt{3}/2$	$-\sqrt{3}$	1
	833	-1.5	$-\sqrt{3}/2$	1	$-\sqrt{3}$
	388	-1.5	$-\sqrt{3}/2$	0	0
	883	-1.5	-4.5	$-\sqrt{3}$	$-\sqrt{3}$
	838	-1.5	$-\sqrt{3}/2$	0	0
453	888	-1.5	-1.5	0	0
	333	-1.5	-4.5	1	1
	833	-1.5	$\frac{3\sqrt{3}}{2}$	1	$\sqrt{3}$
	383	-1.5	$-\frac{3\sqrt{3}}{2}$	$\sqrt{3}$	1
	338	-1.5	-4.5	$-2\sqrt{3}$	$-2\sqrt{3}$
	838	-1.5	$\frac{3\sqrt{3}}{2}$	$-2\sqrt{3}$	0
	883	-1.5	-1.5	$\sqrt{3}$	$\sqrt{3}$
	388	-1.5	0	$-\frac{3\sqrt{3}}{2}$	$-2\sqrt{3}$

Table 1b:The $SU(3)$ color matrix elements of the ghost triangle.

abc	deh	$D_hD_dD_e$	$D_h\phi_d\phi_e$	$D_d\phi_e\phi_h$	$D_e\phi_h\phi_d$
678	888	-1.5	-4.5	0	0
	333	-1.5	-1.5	1	1
	338	-1.5	-1.5	0	0
	383	-1.5	$\sqrt{3}/2$	$\sqrt{3}$	1
	833	-1.5	$\sqrt{3}/2$	1	$\sqrt{3}$
	388	-1.5	$\sqrt{3}/2$	0	0
	883	-1.5	-4.5	$\sqrt{3}$	$\sqrt{3}$
	838	-1.5	$\sqrt{3}/2$	0	0

Table 1c:The $SU(3)$ color matrix elements of the ghost triangle.

abc	dh	$D_h D_d D_{Ae}$	$D_{Ae}\phi_h\phi_d$
321	88	1.5	-1.5
	33	1.5	-4.5
	83	1.5	0
	38	1.5	0
854	88	1.5	-4.5
	33	1.5	-1.5
	83	1.5	$\sqrt{3}/2$
	38	1.5	$\sqrt{3}/2$
876	88	1.5	-4.5
	33	1.5	-1.5
	83	1.5	$-\sqrt{3}/2$
	38	1.5	$-\sqrt{3}/2$

Table 2: The $SU(3)$ color matrix elements of the ghost-ghost-gluon triangle.

a) The ghost loop in the gluon propagator

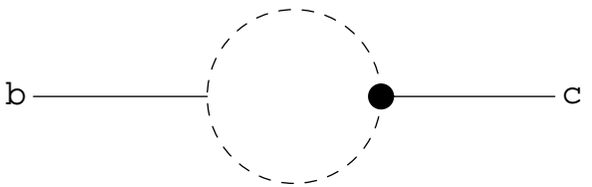

Fig. 9: The gluon propagator dressed by the ghost propagator.

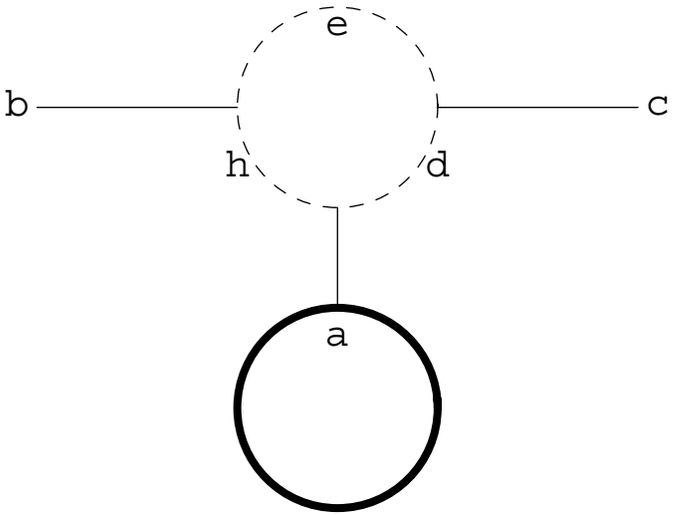

Fig.10: The ghost loop contribution in the gluon propagator. The dashed line represents a ghost and the thick line is a quark.

b) The gh-gh-gl loop in the ghost propagator

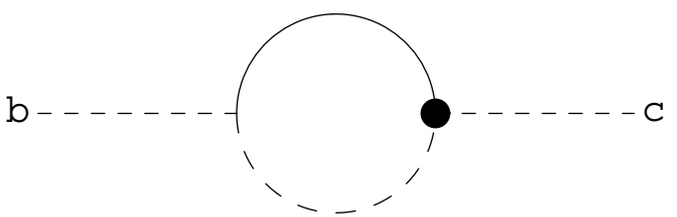

Fig. 11: The ghost propagator.

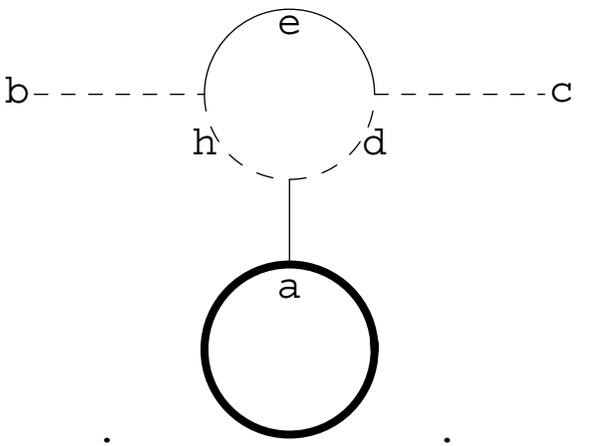

Fig. 12: The dressing of the ghost propagator by the gluon. The dashed line represents a ghost the thin line a gluon, and the thick line a quark.

- Since in the gluon propagator, color indices e,d,h can be rotated, the color index a specified by the quark loop is not necessarily in the Cartan subalgebra. The propagator is proportional to f^{abc}, and since the signs of the color matrix element given in Table 1 are random, its contribution is expected to be small, and thus the gluons propagator is color diagonal.

- In the ghost propagator, color indices h and d can make a color antisymmetric ghost when the index a is in Cartan subalgebra, and thus the ghost propagator is not necessarily color diagonal.

IV. Reconsideration of the Slavnov identity in infrared

$$
\begin{aligned}
Z(j,\chi,\bar{\chi}) &= \int \prod_{x,\nu} dA_\nu(x) d\bar{c} dc \\
&\times \{s_0 + s_{0c} + s_1 + s_2 + s_c - \frac{i}{2\alpha}\int dx (\partial^\mu A_\mu{}^b)^2\} \\
&\times \exp\{i\int dx [j_a^\mu A_\mu^a + \bar{c}\chi^a + \bar{\chi}^a c^a]\}.
\end{aligned}
$$

$$
s_0 = -\frac{i}{4}\int dx (\partial_\mu A_\nu{}^a - \partial_\nu A_\mu{}^a)^2
$$

$$
s_{0c} = i\int dx \partial^\mu \bar{c}^a \partial_\mu c_a
$$

$$s_1 = -igf^{abd}g^{\nu\nu}\int dx(\partial_\mu A_\nu{}^a)A_\mu{}^b A_\nu{}^d$$

$$s_2 = -\frac{ig^2}{4}f^{abd}f^{ab'd'}g^{\mu\mu}g^{\nu\nu}\int dx A_\mu{}^b A_\nu{}^d A_\mu{}^{b'} A_\nu{}^{d'}$$

$$s_c = igf^{abd}\int dx(\partial^\mu \bar{c}_a)A_\mu{}^b c_d$$

- $s = s_1 + s_2 + s_c$, $\bar{S} = e^s = E_0(s)$.
- $\bar{c}^a = \hat{\bar{c}}^a + \check{\bar{c}}^a$, $A^a = \hat{A}^a + \check{A}^a$,
- $\hat{\bar{c}}$: The field serves as an external leg.
- $\check{c}$: The field generates internal lines in the diagram.

- BRST transformation.

$$\begin{aligned}
\delta A_\mu{}^a(x) &= (\partial_\mu c^a(x) + g f^{abd} A_\mu{}^b(x) c^d(x))\epsilon \\
\delta c^a(x) &= \frac{g}{2} f^{abd} c^b(x) c^d(x) \epsilon \\
\delta \overline{c}^a(x) &= -\frac{1}{\alpha} \partial^\mu A_\mu{}^a(x) \epsilon
\end{aligned}$$

- For $F(A_\mu, \overline{c}, c) = A_\mu{}^b \overline{c}^d(y)$ the Slavnov identity implies:

$$\begin{aligned}
&\langle S\delta F \rangle = \frac{1}{\alpha} \langle S A_\mu{}^b(x) \partial^\nu A_\nu{}^d(y) \rangle + \langle S \partial_\mu c^b(x) \overline{c}^d(y) \rangle \\
&+ g f^{bpq} \langle S A_\mu{}^q(x) c^p(x) \overline{c}^d(y) \rangle = 0
\end{aligned}$$

- The Yang-Feldman relation for the interpolating field $\check{\phi}(x)$ in general:

$$\check{\phi}(x) = \phi(x) + \int dy D^{ret}(x-y)\check{J}(y)$$

$$(\Box + m^2)D^{ret}(x) = \delta(x)$$

- Composite field given by monomials of $\phi(x)$ which is expressed by the derivative of renormalized S-matrix $\dfrac{\delta E_0(s_r)}{\delta\phi}$ yields an equation

$$(\Box + m^2)\check{\phi}(x) + i\frac{\delta E_0(s_r)}{\delta\phi(x)} = (\Box + m^2)\phi(x)$$

- Introduce composite fields

$$j_1(x) = -igf^{abd}(\Box_\perp{}^{\mu\nu}\hat{A}_\mu{}^a(x))A_\nu{}^b(x)c^d(x)$$

and

$$j_2(x) = \frac{igf^{abd}}{2}(\Box\hat{\bar{c}}^a(x))c^b(x)c^d(x),$$

which satisfies

$$(j_1 + j_2)\bar{S} = \partial_\mu\hat{c}\frac{\delta\bar{S}}{\delta A_\mu}.$$

$$\Box^{\mu\nu} = g^{\mu\nu}\Box - \partial^\mu\partial^\nu(1 + \frac{1}{\alpha})$$

and $\Box_\perp$ is the transverse part of $\Box^{\mu\nu}$

$$\Box_\perp{}^{\mu\nu} = g^{\mu\nu}\Box - \partial^\mu\partial^\nu.$$

- Slavnov identity

$$\langle S\delta F\rangle = \left\langle \int dx\{\frac{\delta F}{\delta A_\mu{}^a(x)}(\partial^\mu c^a(x) + g f^{abd} A_\mu{}^b(x) c^d(x)) \right.$$
$$\left. -\frac{\delta F}{\delta \bar{c}^a(x)}\frac{1}{\alpha}(\partial^\mu A_\mu{}^a(x)) + \frac{\delta F}{\delta c^a(x)}\frac{g}{2} f^{abd} c^b(x) c^d(x)\} S \right\rangle = 0$$

can be rewritten as

$$\langle F\delta S\rangle = \left\langle F \int dx\{(-i\Box^{\mu\nu}\hat{A}^a_\nu)\partial^\mu c^a - (-i\Box\hat{c}^a)\frac{1}{\alpha}\partial^\nu A_\nu{}^a \right.$$
$$+\frac{i}{\alpha} g f^{abd}(\partial^\mu\partial^\nu)\hat{A}^a_\nu A_\mu{}^b c^d + g f^{abd}(-i\Box^{\mu\nu}_\perp \hat{A}^a_\nu) A_\mu{}^b c^d$$
$$\left. -\frac{g}{2} f^{abd}(-i\Box\hat{\bar{c}}^a) c^b c^d\} S \right\rangle = 0.$$

- Using the relation $\partial_\mu \Box^{\mu\nu} = -\frac{1}{\alpha}\partial^\nu \Box$, the first three terms can be combined to $\frac{1}{\alpha}\partial^\nu A^a_\nu (i\Box \check{c}^a)$.

- The last two terms could be expressed by composite fields $J_1(x)$ and $J_2(x)$ that satisfy

$$\int dx \partial_\mu c^a(x) \frac{\delta S}{\delta A_\mu{}^a(x)} = \int dx (J_1(x) + J_2(x))$$

- Since gluon propagator is color diagonal, $\frac{\delta S}{\delta A_\mu{}^a(x)} = S(-i\Box^{\mu\nu} \check{A}^a_\nu)$

- Since external ghost can couple with internal ghost,
  $\frac{\delta S}{\delta \bar{c}^a(x)} = S[-i\Box \breve{c}^a - igf^{abd}\partial^\mu(A^b_\mu c^d)](x)$
- Although $\frac{\delta \bar{S}}{\delta \bar{c}^a(x)} = -igf^{abd}\partial^\mu(A^b_\mu c^d)(x)\bar{S}$, $(\bar{S} = e^{s_1+s_2+s_c})$
  $\langle S\delta F\rangle = \left\langle \int dx\{-\frac{1}{\alpha}(\partial^\nu \hat{A}^a_\nu)(-i\Box\breve{c}^a) - \frac{i}{\alpha}g(\partial^\nu \hat{A}^a_\nu)\partial^\mu(A_\mu{}^b c^d)f^{cbd}\}S\right\rangle$
  $= 0$ is satisfied only when $\frac{\delta S}{\delta \bar{c}^a(x)} = S(-i\Box\breve{c}^a(x))$, i.e. ghost propagator is color diagonal.
- The external ghost $\partial_\mu \bar{c}^b$ can couple to internal c^d and effectively play the role of $\partial_\mu \bar{c}^a$ in the infrared. (At high energy, color antisymmetric ghost propagator is suppressed.)

- The same argument applys to the theory of t'Hooft. The color antisymmetric ghosts may cancel among themselves in the tree level. But affects physics in the infrared through loops.

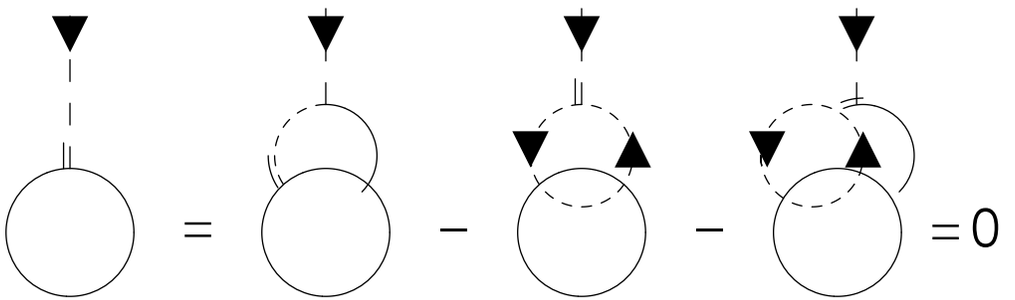

Fig.13:The cancelling mechanism of longitudinal gluon and ghosts.

t'Hooft. Nucl. Phys. **B33**173(1971).

a) Effects on the Kugo-Ojima confinement parameter

- Kugo-Ojima theory (1979): One constructs a two-point function $u^{ab}(q)$ from the Lagrangian in the Landau gauge that satisfies BRST symmetry. If its value at momentum zero is -1, it is an evidence of the the color confinement.

$$(\delta_{\mu\nu} - \frac{q_\mu q_\nu}{q^2}) u^{ab}(q^2)$$
$$= \frac{1}{V} \sum_{x,y} e^{-ip(x-y)} \langle \mathrm{tr} \left(\Lambda^{a\dagger} D_\mu \frac{1}{-\partial D} [A_\nu, \Lambda^b] \right)_{xy} \rangle .$$

$$c = u^{ab}(0) = -\delta^{ab} c$$

- When we define

$$\langle c\bar{c}\rangle \equiv -\frac{1}{q^2 G(q^2)},$$

$$\langle (A_\mu \times c)\bar{c}\rangle_{1PI} \equiv -iq_\mu F(q^2)$$

and

$$\langle D_\mu c\bar{c}\rangle = \langle \partial_\mu c\bar{c}\rangle + \langle (A_\mu \times c)\bar{c}\rangle \equiv iq_\mu(1+F(q^2))\frac{1}{q^2 G(q^2)}, \quad (7)$$

we obtain

$$\begin{aligned} \langle D_\mu c(A_\mu \times \bar{c})\rangle &= \langle \partial_\mu c\bar{c}\rangle\langle c(A_\mu \times \bar{c})\rangle_{1PI} + \langle (A_\mu \times c)(A_\nu \times \bar{c})\rangle_{1PI} \\ &\neq (\delta_{\rho\mu} - \frac{q_\mu q_\rho}{q^2})\langle c(A_\mu \times \bar{c})\rangle_{1PI}. \end{aligned} \quad (8)$$

- Although our finite size lattice simulation suggests $G(0) = 0$, there could be a contribution of the ghost propagator of the type appearing between c and $\bar{c}$ that is not proportional to δ^{ab}. Thus, $1 + u(0) = 1 + F(0)$ is not necessarily equal to 0 and $F(0)$ can deviate from -1.
- In the continuum limit, a solution with $G(0)$ =finite is possible.

  Boucaud et al., arXiv:0801.2721, Oliver Pène

  Then $1 + F(0)$ is not necessarily of higher order 0.

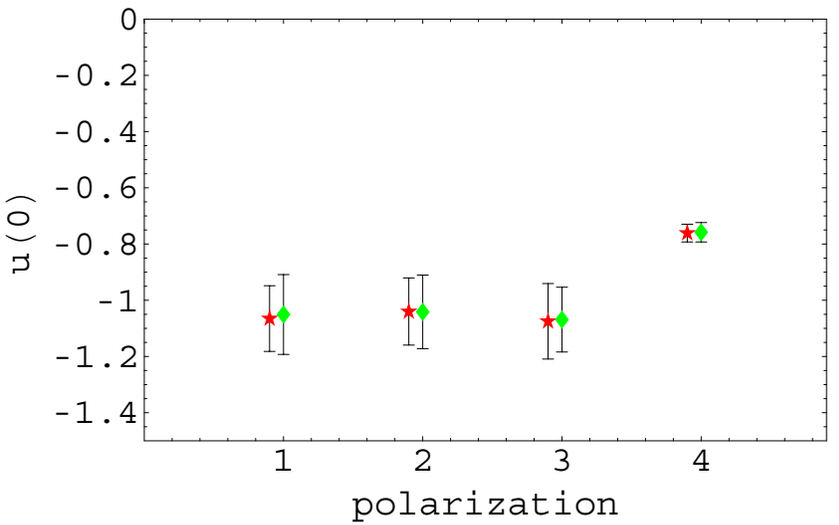

Fig.14: Kugo-Ojima parameter $u(0)$ of MILC$_f$ $N_f = 2+1$ KS fermion unquenched configurations of $\beta_{imp} = 7.11$(green diamonds), $\beta_{imp} = 7.09$(red stars). zero temperature.

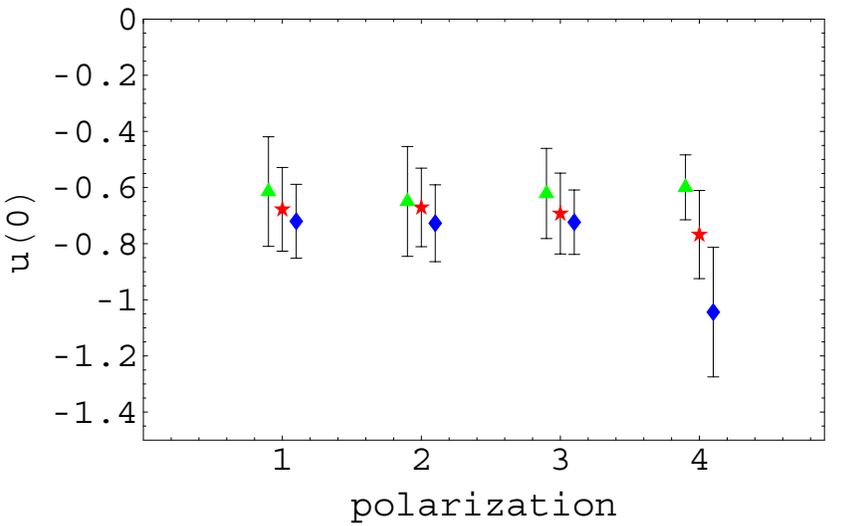

Fig.15: Kugo-Ojima parameter $u(0)$ of MILC$_{ft}$ configurations of $T/T_c = 1.02$(blue diamonds), $T/T_c = 1.23$(red stars) and $T/T_c = 1.32$(green triangles).

The Kugo-Ojima parameter of quenched and unquenched SU(3)

	β_{imp}/β	c_x	c_t	c	e/d	h
quench	6.4			0.827(27)	0.954(1)	-0.12
	6.45			0.814(89)	0.954(1)	-0.14
MILC$_c$	6.76	1.04(11)	0.74(3)	0.97(16)	0.9325(1)	0.03(16)
	6.83	0.99(14)	0.75(3)	0.93(16)	0.9339(1)	-0.00(16)
MILC$_f$	7.09	1.06(13)	0.76(3)	0.99(17)	0.9409(1)	0.04(17)
	7.11	1.05(13)	0.76(3)	0.98(17)	0.9412(1)	0.04(17)
MILC$_{ft}$	5.65	0.72(13)	1.04(23)	0.80(21)	0.9400(7)	-0.14(21)
	5.725	0.68(15)	0.77(16)	0.70(15)	0.9430(2)	-0.24(15)
	5.85	0.63(19)	0.60(12)	0.62(17)	0.9465(2)	-0.33(17)
MILC$_{2f}$	7.20	1.01(13)	0.74(4)	0.94(13)	0.9365(1)	-0.006(130)
MILC$_{3f}$	7.18	1.07(13)	0.76(3)	0.99(16)	0.9425(1)	-0.048(170)

The Kugo-Ojima parameter of the quenched 56^4 lattice and that of the unquenched KS fermion (MILC$_c$,MILC$_f$,MILC$_{ft}$, MILC$_{2f}$ and MILC$_{3f}$). c_x is the polarization along the spatial directions, c_t is that along the time direction, c is the average of c_x and c_t, e/d is the trace divided by the dimension and h is the horizon function deviation.

b) Effects on the QCD running coupling

- In Coulomb gauge, there is a coupling constant $\alpha_I(\boldsymbol{q}^2)$

$$\boldsymbol{q}^5 D_G(\boldsymbol{q})^2 D_A(\boldsymbol{q}) \propto \alpha_I(\boldsymbol{q}^2).$$

- In Landau gauge the coupling constant is $\alpha_s(q^2)$.

$$q^6 D_G(q)^2 D_A(q) \propto \alpha_s(q^2).$$

- gluon : $D_A(q^2) \sim (qa)^{-2(1+\alpha_D)}$
- ghost : $D_G(q^2) \sim (qa)^{-2(1+\alpha_G)}$
- Effective potential from fluctuation in the deep IR: $3\alpha_D - 2\alpha_G < -2$. Braun,Gies,Pawlowski,arXiv:0708.2413
- The fixed point scenario suggests $\alpha_D + 2\alpha_G = 0$

- Conformal theory suggests $\alpha_s(0) = 3.1$. Brodsky, Deur, von Smekal
- Paris solution $\alpha_D = -1, \alpha_G = 0$, (+vertex correction $\kappa = 1$)
- Graz solution $\alpha_D = -1.2, \alpha_G = 0.6$. Schwenzer, Alkofer

	β_{imp}	α_G	α_D	$\alpha_D + 2\alpha_G$	$3\alpha_D - 2\alpha_G$
MILC$_c$	6.76	0.25	-0.60	-0.10	-2.30
	6.83	0.23	-0.57	-0.11	-2.17
MILC$_f$	7.09	0.24	-0.67	-0.19	-2.49
	7.11	0.23	-0.65	-0.19	-2.41

The QCD running coupling

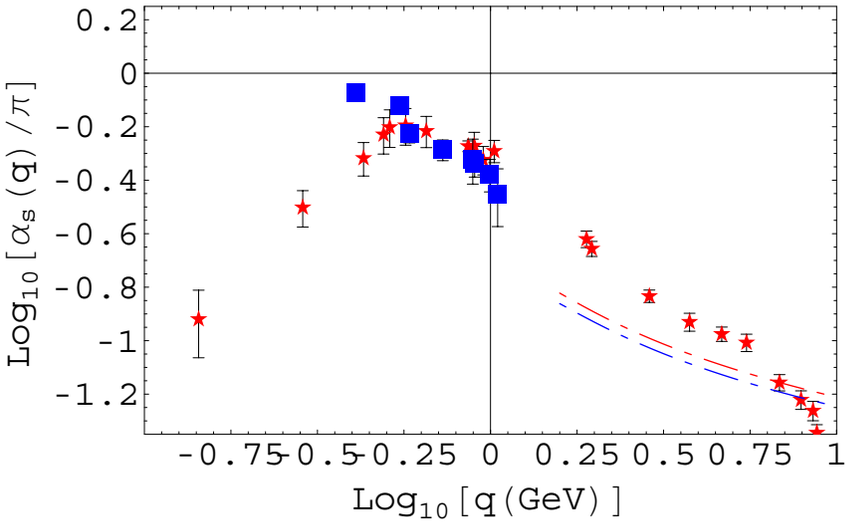

Fig.16:The running coupling $\alpha_s(q)/\pi$ of MILC$_f$ in Landau gauge The pQCD result of $N_f = 3$ (upper dash-dotted line) and $N_f = 2$ (lower dashed line) and the extraction of JLab are also plotted(blue boxes).

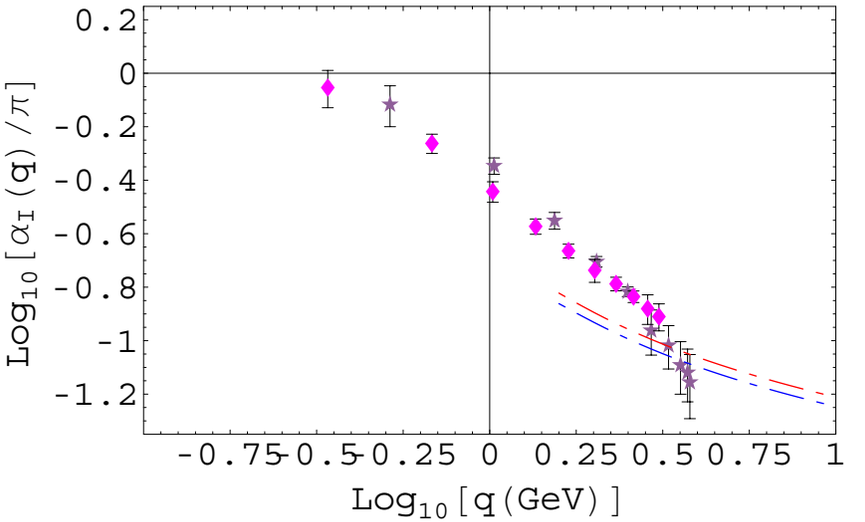

Fig.17:The running coupling $\alpha_I(q)/\pi$ of MILC$_{3f}$ and MILC$_{2f}$ in Coulomb gauge. The pQCD result of $N_f = 3$ (upper dash-dotted line) and $N_f = 2$ (lower dashed line) are also plotted.

V. Some results from the DWF quark propagator

- The mass of a DWF is given by the bare mass sitting on the domain wall $m_f Q^{(w)}$ and the mid-point matrix $Q^{(mp)}$ where the chirality mixing occurs.

$$Q^{(w)}_{s,s'} = P_L \delta_{s,0} \delta_{s',0} + P_R \delta_{s,L_s-1} \delta_{s',L_s-1}$$

$$Q^{(mp)}_{s,s'} = P_L \delta_{s,L_s/2} \delta_{s',L_s/2} + P_R \delta_{s,L_s/2-1} \delta_{s',L_s/2-1}$$

- The conjugate gradient method chooses a solution on the stable manifold among chaotic environment.

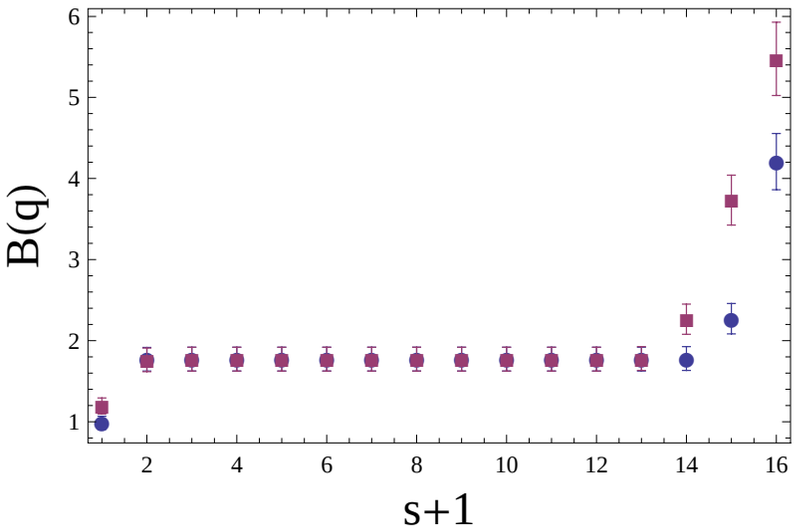

Fig.18:The numerator $\mathcal{B}_{L/R}(2N_c)$ of the mass function of DWF $m_f = 0.01/a$ (blue disk/red box). $\bar{q} = (0,0,0,0)$.

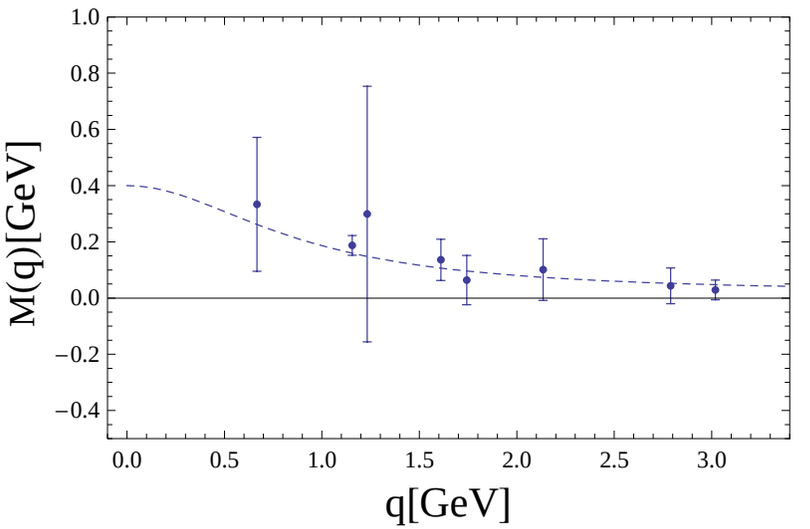

Fig.19:The mass function of the domain wall fermion. $m_f = 0.01/a$. (149 samples)

VI. Summary and discussion

- Color antisymmetric ghost introduces a fluctuation in the one loop level.
- Quark has the effect of magnifying the square norm of the color antisymmetric ghost propagator and reduces its fluctuation.
- Lattice simulations suggests a complicated structure of the infrared fixed point.
- The infrared suppression of $\alpha_s(q)$ in the Landau gauge may be due to the singularity of the color antisymmetric ghost propagator that disturbs the color diagonal part.

- Confinement occur through magnetic fluctuation, and the modulus of color antisymmetric ghost is stabilized by dynamical quarks.
- Chiral symmetry and confinement are related.
- The DWF quark propagator is obtained as a solution on the stable manifold in the chaotic environments using the conjugate gradient method.
- More extensive momentum dependence of the Coulomb gauge DWF quark propagator will be studied.

Thanks

References

[1] T. Kugo and I. Ojima, Prog. Theor. Phys. Suppl. **66**, 1 (1979).

[2] V.N. Gribov, Nucl. Phys. **B 139**1(1978).

[3] G. 't Hooft, Nucl. Phys. **B33**(1971), 173.

[4] J.C. Taylor, Nucl. Phys. **B33** (1971), 436.

[5] O.I. Zavialov, *Renormalized Quantum Field Theory*, Kluwer Academic Pub. (1990)

[6] S. Furui, Prog. Theor. Phys.**119**, 149 (2008)

[7] S. Furui and H. Nakajima, Braz. J. Phys.**37**, 186 (2007), arXiv:hep-lat/0609024.

[8] S. Furui and H.Nakajima, Phys. Rev. D**69**,074505(2004), hep-lat/0305010.

[9] S. Furui and H.Nakajima, Phys. Rev. D**70**,094504(2004), hep-lat/0403021.

[10] S. Furui and H. Nakajima, Few-Body Systems **40**,101 (2006), hep-lat/0503029.

[11] S. Furui and H. Nakajima, Phys. Rev. D**73**,074503(2006),hep-lat/0511045.

[12] S. Furui and H. Nakajima, Phys. Rev. D**73**,094506(2006),hep-lat/0602027.

[13] A. Deur et.al., Phys. Lett. B**650**,244 (2007).

[14] A. Cucchieri, T. Mendes and A. Mihara, Phys. Rev. D**72**,094505(2005).

[15] Ph. Boucaud, J-P.Leroy, A. Le Yaouanc, J. Micheli, O. Pène, J. Rodriguez-Quintero, arXiv:0801.2721[hep-ph].

[16] J. Braun, H. Gies and J. M. Pawlowski,arXiv:0708.2413

[17] S.J. Brodsky and H.J. Lu, Phys. Rev. D**51**,3652 (1995).

[18] S.J. Brodsky, S. Menke, C. Merino and J. Rathsman, Phys. Rev. D**67**, 055008 (2003).